



Fermi National Accelerator Laboratory

FERMILAB-Conf-94/356-E

Neutrino Optics

David C. Carey

Fermi National Accelerator Laboratory

P.O. Box 500, Batavia, Illinois 60510

October 1994

Presented at the *Fourth International Conference on Charged Particle Optics. Tsukuba, Japan, October 2-6, 1994*

Disclaimer

This report was prepared as an account of work sponsored by an agency of the United States Government. Neither the United States Government nor any agency thereof, nor any of their employees, makes any warranty, express or implied, or assumes any legal liability or responsibility for the accuracy, completeness, or usefulness of any information, apparatus, product, or process disclosed, or represents that its use would not infringe privately owned rights. Reference herein to any specific commercial product, process, or service by trade name, trademark, manufacturer, or otherwise, does not necessarily constitute or imply its endorsement, recommendation, or favoring by the United States Government or any agency thereof. The views and opinions of authors expressed herein do not necessarily state or reflect those of the United States Government or any agency thereof.

Neutrino Optics

David C. Carey

Fermi National Accelerator Laboratory*
Batavia, Illinois 60510 U.S.A.

Abstract

Neutrinos are produced by the in-flight decay of π and K mesons. Neutrinos are uncharged and cannot be focused directly. However, the transverse momentum of the neutrino due to the decay is typically much smaller than the transverse momentum spread of the parent meson. The focusing of the meson beam will then significantly enhance the neutrino flux at a distant detector.

Neutrino beams can effectively be focused in the same manner as other charged particle beams, by means of quadrupoles and bending magnets. The bending magnets also can serve to define the momentum of the neutrino beams. Alternatively, neutrino beams can be focused by the use of magnetic horns. Both systems are described here.

Proposed experiments with neutrinos to detect neutrino oscillations place the detector hundreds of kilometers away from the source. The flux of neutrinos through the detector then becomes very small. The calculation of the flux by conventional Monte Carlo or numerical integration techniques becomes prohibitively difficult. A alternate mathematical technique can be used to give results which are reliable to about 10 %

The Production of Neutrinos

Neutrinos are produced by the in-flight decay of π and K mesons. Figure 1 is a schematic diagram of a neutrino facility.

At Fermilab, the proton beam is extracted from the accelerator, split into several smaller beams, and transported out to the experimental areas. One of these areas is the neutrino laboratory, where experiments using neutrinos are performed.

There the proton beam strikes a 30 cm beryllium oxide target. As the protons pass through the target, they suffer collisions with the nuclei of the atoms of the target, creating showers of mesons and other particles. The mesons then enter an evacuated pipe one meter in diameter and 400 meters long. As the mesons travel down this cylindrical cavity, they decay, producing muons and neutrinos.

Actually π^+ and K^+ mesons produce antimuons and neutrinos, and π^- and K^- mesons produce muons and antineutrinos. For pions the branching ratio to the two body mode including a neutrino is essentially 100 % . For kaons it is 63.5 % . The characteristic length for the decay is 56 meters per GeV for pions and 7.5 meters per GeV for kaons. For a

given meson momentum, the neutrinos are uniformly distributed in energy from zero to a maximum of rp where p is the meson momentum. The coefficient r is given in terms of the mass of the meson m and that of the muon μ , by

$$r = \frac{m^2 - \mu^2}{m^2} \quad (1)$$

For pions the value of r is .427, while for kaons it is .954.

At the end of the pipe is the beginning of an earth berm one kilometer long. The function of the berm is to eliminate all the particles except for the neutrinos. The mesons, neutrons, protons and their antiparticles will suffer nuclear collisions and be absorbed in the first few meters of the berm. Muons do not experience the strong interaction, and therefore lose energy gradually through various electromagnetic interactions.

The length of the Fermilab berm was designed to stop muons with a maximum energy of 200 GeV. Since the accelerator now regularly goes to 800 or 900 GeV, the berm has had to be hardened to the muons by the insertion of 20 meters of lead and 140 meters of steel shielding.

Neutrinos experience neither the strong nuclear interaction nor the electromagnetic interaction, but instead interact only by the weak nuclear interaction (the interaction responsible for nuclear beta decay). The neutrino beam will therefore emerge essentially undiminished from the back end of the berm. The only contamination will be a small number of muons created by occasional neutrino interactions in the last few meters of the berm.

The Need for Focusing

Since neutrinos interact only weakly, the fraction of neutrinos that suffer an interaction in the experimental apparatus will be small, even for the most massive of detectors. It is to the experimenter's advantage then to enhance the flux of neutrinos through the detector as much as possible.

The length of the decay pipe has been optimized so that as it is further lengthened the advantage of gaining more decay space is mostly compensated by moving the detector farther away from the decays occurring in the first part of the pipe. The length of the berm is dictated by economics. Originally it was entirely composed of earth. As the energy of the accelerator was upgraded, the berm was hardened by the insertion of lead and steel.

A third possibility is to target as many protons as possible in the neutrino beam. This practice is what is usually done. The neutrino beam is usually a proton hog in any accelerator complex of experimental areas.

The final possibility is to do some kind of focusing, so as to concentrate the existing flux of neutrinos on the detector. The focusing of a neutrino beam has two obvious difficulties:

1. Neutrinos are uncharged and do not experience electromagnetic interactions. There is no practical means of focusing them directly.

2. The neutrino makes a nonzero angle from the original meson direction. The azimuthal angle is randomly distributed about the meson direction. We must be certain that the effect of the decay angle is not to wash out any focusing effect.

The angle between the original meson direction and the neutrino direction is labelled ϕ and is given in terms of the meson momentum p and mass m and the neutrino energy E_ν by

$$\phi = \frac{m}{p} \sqrt{\frac{rp}{E_\nu} - 1} \quad (2)$$

The angle ϕ is shown in figure 2. Holding fixed the neutrino energy, we can consider the angle ϕ as a function of meson momentum. The threshold or minimum meson momentum p necessary to produce a neutrino of energy E_ν is equal to E_ν/r . Below that momentum, the angle ϕ is undefined. The maximum angle occurs at $p = 2E_\nu/r$ and is given by:

$$\phi_{max} = \frac{mr}{2E_\nu} \quad (3)$$

The maximum neutrino transverse momentum from the decay is 30 MeV for pions and 236 MeV for kaons. Most of the useful neutrino flux, as we shall see, comes from decay angles which are somewhat smaller.

The transverse momentum distributions of the pions and kaons produced by 100 GeV protons are shown in figure 3 [1]. The longitudinal momentum distributions for 175 GeV incident protons are shown in figure 4. The incident energies of the protons are different in the two graphs since reference [1] did not have a graph showing the transverse distribution for 175 GeV incident protons. For the purpose for which we are using these graphs the difference in incident proton energy is unimportant. We will refer to the transverse distributions immediately below. We will need to consider the longitudinal distributions a little later in the discussion.

The transverse momentum dependence of the differential cross section for the production of mesons is rather insensitive to the energy of the incoming particle. Most of the dependence comes at transverse momenta far above any shown in figure 3, and can be interpreted as a phase space effect due to the approach to the kinematic boundary. Any conclusions we draw from figure 3 will then be likely to be valid for higher energy protons as well.

The mean value of the transverse momentum of the proton-produced mesons tends to be about 0.4 GeV/c. This value is over ten times the maximum transverse momentum acquired by the neutrino due to the pion decay process. It is also about twice that for the kaon-produced neutrinos. The ratios would be several times larger if the average decay angles were used instead of the maxima.

The spread in direction of the neutrino trajectories has a much greater contribution from the spread in meson direction than from the change in direction due to the decay kinematics. It is therefore to our advantage to focus the mesons. The flux of neutrinos through the particle detector will then be enhanced.

The situation is still different from that of a stable particle beam. It is not completely obvious that the most desirable thing to do is to point the meson trajectories directly at the detector. For a given neutrino energy E_ν , the variation of the decay angle ϕ with meson momentum p is most rapid at threshold. If the meson trajectory is directed at the center of the detector, the neutrino cone at the detector position may quickly grow large enough so that it is totally outside the detector. It might be better to point the mesons a slight distance away from the detector, so that, as the decay cone grows, it sweeps across the detector at a meson momentum where the decay angle ϕ is varying more slowly.

To evaluate this question, let us consider a detector area sufficiently small so that we can make linear approximations in evaluating the neutrino flux through it. We need consider only two cases

1. The projected meson trajectory points at the very center of the detector
2. The projected meson trajectory lies outside of the detector.

The other obvious case, where the projected meson trajectory lies inside the detector but is not at its center can easily be eliminated by making the detector smaller. Then the projected meson trajectory can be made to lie outside the detector. The number we shall evaluate, which we shall call ΔF , is the fraction of the neutrino cone which strikes the detector integrated over momentum. We consider the meson direction to be held constant, while the momentum is increased. If the area of the detector is ΔA , then for the projected meson trajectory at the center of the detector, we have.

$$\Delta F = \frac{\Delta A}{\pi m^2} \left(\frac{E_\nu}{r} \right)^3 \quad (4)$$

If the meson trajectory is pointed outside of the detector, this expression becomes

$$\Delta F = \frac{\Delta A}{\pi m^2} p^3 \left(\frac{1}{2 - \frac{rp}{E_\nu}} \right). \quad (5)$$

We can see that this expression reduces to the one in equation (3) when the meson momentum is just at threshold, which is what occurs when the meson trajectory points at the center of the trajectory. There is no great advantage on the basis of geometry of favoring an exact hit over a near miss. It is sufficient that the cone intersect the trajectory for some meson momentum.

The expression for ΔF becomes singular for a meson momentum of twice the threshold. However, this corresponds to the maximum decay angle when the meson momentum is twice the threshold. Linearization obviously is not a good approximation at this meson momentum. As we shall see below, for a given neutrino energy the contribution from this portion of the meson momentum range is unimportant.

If we now examine figure 4, we see that the meson cross section is falling rapidly with longitudinal momentum. The invariant differential cross section can be parameterized as being proportional to $(1 - x)^n$, where x is the fraction that the meson longitudinal momentum constitutes of the original proton momentum and n is an index which depends on the type of meson. The values from reference [1] are given in the following table:

π^+	3.4
K^+	2.6
π^-	4.4
K^-	4.6

Geometry matters little in selecting the meson momentum contributing most strongly to a given neutrino energy. However, meson production dynamics matters a great deal. The mesons are produced most copiously just above the threshold for the neutrino energy. Therefore, in our discussion of focussing devices, our design goal will be to point the meson trajectories at the detector.

Focusing Devices

Horns

A neutrino horn [2] [3] is shown in figure 5. It is constructed from a thin sheet of copper which is wrapped into a tube of varying diameter. The tube is of smallest diameter near the longitudinal midpoint, and is significantly larger at both ends. It is therefore a rotationally symmetric device with the axis of symmetry along the axis of the decay pipe. A focusing system may have one, two, or three horns. The production target for the mesons is on the same axis. It is often located just before the entrance to the first horn of the system.

An electrical current is passed longitudinally through the horn. This creates a magnetic field whose field lines are along circles whose centers are along the horn axis and are perpendicular to the horn axis. The strength of the field B is given in terms of the horn current I by:

$$B = \frac{\mu_0 I}{2\pi r} \quad (6)$$

The field strength is then inversely proportional to the distance r from the axis of the horn.

The magnetic field is contained entirely outside of the inner surface of the copper sheet comprising the horn. Mesons passing through the neck of the horn experience no field. The particles enter the field by penetrating through the copper sheet at the front of the horn. They are then focused by the field of the horn and subsequently pass through the copper once more in exiting through the back of the horn.

Some of the mesons will be stopped by nuclear interactions in the horn. The copper must therefore be kept as thin as possible. However, the thinness of the copper exacerbates any heating problem since a large current density is necessary to create a magnetic field of a given strength. Horns are therefore operated in pulsed mode. A current of a few tenths of a megamp is typically passed through the horn for a few hundred microseconds. The

accelerator must then operate in a mode where large numbers of protons are extracted in a similar time period.

In the previous section we discussed the fact that the production of mesons is limited in transverse momentum in a manner that was relatively independent of longitudinal momentum. This dynamical situation has the result that the peak production of mesons of different momenta occurs at different angles. The smaller the momentum of the meson the larger the angle of peak production. Different regions of the horn can then be designed to focus different momenta. The horn is a broad-banded device, designed to maximize the flux over a large range.

Horns are designed with a certain degree of trial and error. The entrance and exit surfaces can be contoured so that the focusing is point to parallel throughout the horn, where each momentum is focused at its maximum production angle. Since any neutrino detector is much larger in diameter than either the horn or the decay pipe, point to parallel focusing is essentially the same as point to point.

When two or more horns are used, their focusing characteristics are somewhat independent. The hole in the second horn will be larger than that in the first horn. However the second horn is sufficiently far from the target that the solid angle subtended by the hole is significantly smaller for the second horn. The first horn focuses particles through the hole of the second horn. The second horn then focuses particles which passed through the hole of the first horn. If a third horn is used, the process is simply extended. Once again, the final design is often arrived at by trial and error. Some trajectories inevitably pass through two or more horns.

A Quadrupole Triplet

Experiments involving wire chambers and studying coincidences or doing event reconstruction will need to have events well separated in time. Under such circumstances it is necessary to have the particles removed from the accelerator and transported to the production target in a time period of several seconds.

Since the horn is a pulsed device, it would not be suitable to a long spill situation. For this reason conventional quadrupole triplet [4] is used. A triplet configuration which has been used at Fermilab [5] is shown in figure 6.

The triplet is focused point to parallel [6] for 300 GeV mesons. Because of chromatic aberration, the triplet cannot be as broad banded a device as the horn. Because of aperture limitations, the flux even at a given momentum cannot be as great. However, the number of experiments at Fermilab demanding a long spill beam is sufficiently great that the quadrupole triplet has received much use.

A Dichromatic Beam

For some experiments it is desirable to know the neutrino energy. Since 1973 [7] it has been known that neutrinos can interact via two mechanisms, known as "charged current"

and “neutral current.” In a charged current interaction, the incident neutrino exchanges a W particle (which is charged) with a nucleon and transforms itself into a muon. The muon is charged and its energy can be determined by magnetic deflection. The energy of the hadronic products of the reaction can be determined by calorimetry. Knowledge of the neutrino energy can add to the certitude of the measurements, but is not a missing ingredient.

The neutral current interactions occur via the exchange of a neutral particle with the designation Z^0 . The neutrino then is not transformed to a charged lepton but remains as a neutrino, although with some energy loss. The neutrino is then lost as the chances that it will interact again in the experimental apparatus are very slim indeed. Other means must be used to estimate the incident neutrino energy.

In ordinary charged particle optics [4], a magnetic channel can be designed to select a single momentum. Bending magnets, quadrupoles, and slits are arranged so that the particles emerging from the end of the beam line have a small spread about the selected momentum.

In neutrino optics the same selection can be made on the meson momentum. However the energy of the neutrinos produced in the forward direction will depend on the type of meson. As noted above, the neutrinos will have 42.9 % of the meson energy for pions and 95.4 % for kaons. The result is then a dichromatic beam, with two energy peaks.

A diagram of the Fermilab dichromatic neutrino beam [8] [9] is shown in figures 7 and 8. The quadrupoles focus the beam from point to parallel in both transverse planes. The first set of bends deflects the beam horizontally, while the second set deflects it vertically. Since the detector is large, the beam does not need to be recombined in position, but only in angle. The two sets of bends therefore do not need to bend in the same plane.

In fact it is imperative that the two sets of bends bend in different planes. Neutrinos will be produced by the mesons at all points along their trajectories. This includes the part of the trajectory within the magnetic channel. The neutrinos are not constrained by the apertures of the magnetic channel. If the beam at any intermediate point is pointed at the detector, there is a substantial increase in the background, thus compromising the dichromatic nature of the beam. In the Fermilab dichromatic neutrino beam design, the background is minimized by having the beam not point at the detector except at the downstream end.

Flux Calculations

A calculation of the flux must include both the desired particles and the background. Since the neutrinos pass right through the iron of the magnets or the copper of the magnet coils or the horns we must consider the decay of mesons anywhere it might occur. The neutrinos can be produced before the focusing system, inside it, or after the focusing system inside the decay tunnel. We must follow the meson trajectories from their origin in the target until they are stopped by hitting an aperture in the focusing system, or the side or end of the decay pipe.

The mesons are produced over an energy range that can be quite broad. At Fermilab, we frequently consider meson momentum ranges from zero to 900 GeV/c. The angular range

may be as small as 8 milliradians for high energy neutrino calculation, or as large as 50 milliradians for lower energy. To calculate the flux, we must cover the entire range in both momentum and production angle.

At each combination of momentum and angle, we must trace a representative trajectory through the focusing system and down the decay pipe. We must consider the possibility of decay at any point along the meson trajectory. When the meson decays, the neutrino energy may vary from zero up to a factor r , explained above, times the meson momentum. For a given meson momentum p , each neutrino energy E_ν will correspond to a certain decay angle ϕ , as given in equation (3). The azimuthal angle can also vary over a range of 360° .

The detector can be quite far away from the place where the decays occur. The berm at Fermilab is one kilometer long. However in figure 9 we see another proposed situation where the detector is quite removed from the source of neutrinos. Such a layout is used to search for neutrino oscillations, which, in theory, will occur should one or more of the three types of neutrino has a nonzero mass.

If we look at figure 10, we see the functional dependence of the decay angle ϕ on meson momentum p for a fixed neutrino energy E_ν . Because the expression for ϕ involves a square root, the derivative of ϕ with respect to p becomes infinite as the threshold value of p is approached from above. At this point the value of ϕ is varying very rapidly. Any calculation based on stepping through the various kinematic variables could easily miss this region and therefore badly misestimate the neutrino flux.

Because of the dimensions involved in the physical layout and the rapid variation of kinematic variables, traditional approaches to the problem of flux calculation based on either a fixed scheme of division of the ranges of the various variables or on Monte Carlo are not of much use. Attempts to use such methods give results where the results calculated may be unreliable by several factors of ten. Instead we must resort to a different approach.

We begin by forming a grid in the space of production momentum and angle. The total momentum interval is divided into a number of bins m , each of width Δp . The total angle interval is divided into a number of bins n , each of width $\Delta\theta$. In the two kinematic variables, we then have a total of mn bins of area $\Delta p\Delta\theta$.

If the production target, focusing system, and decay pipe form a rotationally symmetric system, then the azimuthal angle for the production is ignored as being irrelevant. If the system is not rotationally symmetric, we divide the azimuthal angle ψ into intervals also. We consider a single quadrant, two quadrants, or all four quadrants depending on the symmetry of the beam line.

We step over the production kinematic variables, selecting the values in the bin center as the starting variables for a meson trajectory. The trajectory is traced through the focusing system and down the decay pipe until it is stopped. The trajectory can be stopped by some aperture within the focusing system, or by the side or the end of the decay pipe.

The tracing of the trajectory through the horn is done by a simple numerical integration.

The horn is specified as being bounded by a succession of joined line segments. The shape is not analytically regular, so no sophisticated numerical integration scheme would be appropriate. The ray tracing through a system of quadrupoles and bending magnets is done via standard methods described elsewhere [10].

The trajectory is segmented longitudinally at regular intervals and at the transition into and out of any magnetic element. The number of mesons which decay in each longitudinal segment is calculated and the decay point is taken at the longitudinal midpoint of the segment.

At this point, the straightforward method would be to calculate the decay angle ϕ from the momentum p at the bin center. From that one could calculate the fraction of the decay cone which intersects the detector. This fraction would be taken as equal to the fraction of the neutrinos which hit the detector and are produced by decays in the given longitudinal segment of the meson trajectory. However, since the decay angle ϕ is so rapidly increasing at threshold for a given neutrino energy E_ν , an accurate calculation would require extremely fine binning for the meson momentum.

Instead we take the meson momentum p as being fixed at the bin center only for purposes of tracing the particle trajectory. For calculating the decay geometry, we now take the meson momentum to represent the momentum interval Δp over the entire bin. We hold the position and direction of the meson as fixed and consider what happens as the momentum is varied over Δp .

If the threshold is in the bin, the decay angle will not be defined for the momentum below threshold. After threshold is reached ϕ will increase rapidly, and reach maximum at twice threshold. After maximum, ϕ will decrease slowly.

In figures 11, 12, and 13, we see the various possibilities for the relative positions of the detector and the projection of the decay angle ϕ on the detector plane, in the case when the projected meson direction is inside the detector. The angle subtended by the detector radius is designated as b , and the angle separating the centers of the two circles is s .

If the maximum value of ϕ is less than $s - b$, the neutrino decay cone will be entirely contained within the detector as seen in figure 11. If the maximum value of ϕ is between $s - b$ and $s + b$, then the neutrino cone will again initially be contained entirely within the detector. As the momentum p increases in value the cone will grow until it intersects the detector only partially as seen in figure 12. After its maximum, the cone will begin to shrink and eventually be again entirely contained within the detector.

If the maximum value of ϕ is larger than $s + b$, the angle ϕ will again initially expand and pass through the two stages described above. Eventually it will grow sufficiently large so that none of the decay cone is contained in the detector as seen in figure 13. After maximum, ϕ will again decrease and eventually the cone will again be entirely within the detector.

The fraction of the decay cone intersecting the detector as a function of momentum is shown in figure 14. Only the portion of the function from the increase in ϕ is shown. The

fraction is equal to unity until the angle ϕ becomes large enough so that the decay cone touches the perimeter of the detector. It then rapidly decreases, becoming zero when the opposite side of the cone becomes tangent to the perimeter of the detector. The part from the decreasing portion of ϕ occurs sufficiently slowly that it does not appear on the graph with the scale used.

In figures 15, 16, and 17, we see the various possibilities for the relative positions of the detector and the neutrino cone in the case where the projected meson direction is outside the detector. Now the value of s is smaller than b .

If the maximum value of ϕ is less than $b - s$, the neutrino decay cone will have no intersection with the detector as seen in figure 15. If the maximum value of ϕ lies between $b - s$ and $b + s$, then the neutrino cone will still initially lie entirely outside the detector. As the momentum p is increased, the cone will expand so that it intersects the detector as seen in figure 16. At no point will the cone be entirely within the detector. At most it can approach being half contained within the detector. After its maximum value ϕ will decrease and eventually again have no intersection with the detector.

If the maximum value of ϕ is larger than $s + b$, then the cone will again initially be outside the detector. It will expand to have an intersection with the detector as seen in figure 15. As p is increased, the cone will continue to expand until it contains the detector but has no intersection with it as seen in figure 17. From the maximum value, ϕ will decrease, so that the cone once again intersects the detector, and finally becomes small enough so that there is no intersection.

The fraction of the decay cone intersecting the detector as a function of momentum for this case is shown in figure 18. Only the portion of the function from the increase in ϕ is shown. The fraction is equal to zero until the angle ϕ becomes large enough so that the decay cone touches the perimeter of the detector. It then rapidly increases to a maximum and subsequently decreases to zero. Once again, the portion of the graph where the angle ϕ is decreasing is omitted.

In the behavior, described above, of the decay angle ϕ with momentum p , we can define certain critical momenta. These critical momenta all occur in the region of p where ϕ is increasing. If the center of the decay cone lies within the detector, then the critical points occur at threshold E_ν/r , when the cone first touches the detector perimeter, and when it last touches the same perimeter. If the center of the cone lies outside the detector, then in addition to these three critical points, we include the momentum at which the fraction of the cone intersecting the detector is maximized. In the momentum region above where the maximum of ϕ occurs, the variation of ϕ with momentum is sufficiently slow that no subdivision of the momentum bin Δp is necessary.

If any of these critical momenta lie within the momentum interval Δp , then that momentum interval is subdivided by the critical momenta. The angle ϕ is calculated from the momentum p at the midpoint of each subinterval. From this value of ϕ , the fraction of the cone intersecting the detector is calculated and multiplied by the fraction that the

subinterval comprises of the entire interval Δp . Since the production spectrum varies with momentum p , adjustments are made for such variation. The contributions from the various subintervals are summed to obtain the contributions for the entire interval Δp . The process is repeated for each neutrino energy E_ν , at which the flux is to be calculated.

If the focusing system contains bending magnets and we are considering a high-energy beam, then the effect of meson direction on neutrino direction may be greater than the effect of the variation of the decay angle ϕ with momentum p . In such a case, we calculate the decay angle ϕ from the center of the momentum bin Δp . We calculate certain critical angles as the meson passes through the bending magnet, thereby causing the decay cone to sweep across the detector plane. The contributions to the flux are calculated in a manner similar to what is described above.

The contributions from the longitudinal segments are then added to obtain the contribution to the neutrino flux through the detector for the entire trajectory. If the target and focusing system configuration is not rotationally symmetric, the azimuthal bins are summed to obtain the result for a single $\Delta p \Delta \theta$ bin. The contribution for the $\Delta p \Delta \theta$ bin is multiplied by the meson production spectrum. The results are summed over all bins to obtain the total flux. Runs can be made for both pions and kaons, and the results summed. The neutrino flux plotted as a function of neutrino energy is shown in figure 19. The system used to calculate the flux is the dichromatic beam described above. In general, from comparisons with other methods in simple cases, and consistency checks, the accuracy of the calculation has been found to be on the order of 10 % . Making the grid of kinematic variables more refined will, of course, produce greater accuracy.

The energy resolution is not as bad as it appears to be in the graph. The higher energy neutrinos involve smaller decay angles. Therefore, the neutrino energy will be strongly related to transverse position in the detector. Neutrinos from pions and kaons will separate into two bands in a plot of detector radius vs neutrino energy. An illustration of the scattering of neutrino events can be seen in figure 20. The pion and kaon populations are clearly separated. If, for example, a neutral current event shows a hadron energy greater than 400 GeV, then the neutrino initiating the event came from kaon decay. From the transverse position of the interaction in the detector the incident neutrino can be estimated to greater accuracy than just from the distribution in figure 18. The more accurate neutrino energy estimate can then be used in the analysis of neutrino physics.

References

* Operated by Universities Research Association, Inc., under contract with the United States Department of Energy.

1. A. E. Brenner et al., Physical Review D26, 1497 (1982).
2. F. A. Nezrick, Fermilab Neutrino-Horn Focusing System, Fermilab Internal Report TM-555, 1975.
3. R. Bernstein et al., Conceptual Design Report: Main Injector Neutrino Program

- (1991).
4. D. C. Carey, *The Optics of Charged Particle Beams*, Harwood Academic Publishers, New York, 1987.
 5. A. Skuja, R. Stefanski, and D. Theriot, The 300 GeV Triplet Train, Fermilab Internal Report TM-646 (1976).
 6. K. L. Brown, F. Rothacker, D. C. Carey, and Ch. Iselin, TRANSPORT, A Computer Program for Designing Charged Particle Beam Transport Systems, SLAC Report No. 91 (1977) (revised version to be published soon).
 7. F. J. Hasert et al., Physics Letters B46, 121 (1973).
 8. L. Stutte, A Possible Dichromatic Neutrino Beam for a 1 Tev Accelerator, Fermilab Internal Report TM-841 (1979).
 9. L. Stutte, Further Design Studies for a Tevatron Era Dichromatic Beam - The NCI Dichromatic Beam, Fermilab Internal Report TM-1091 (1982).
 10. D. C. Carey, K.L. Brown, and Ch. Iselin, DECAY TURTLE, A Computer Program for Simulating Charged Particle Beam Transport Systems, Including Particle Decay, SLAC Report No. 246 (1982).

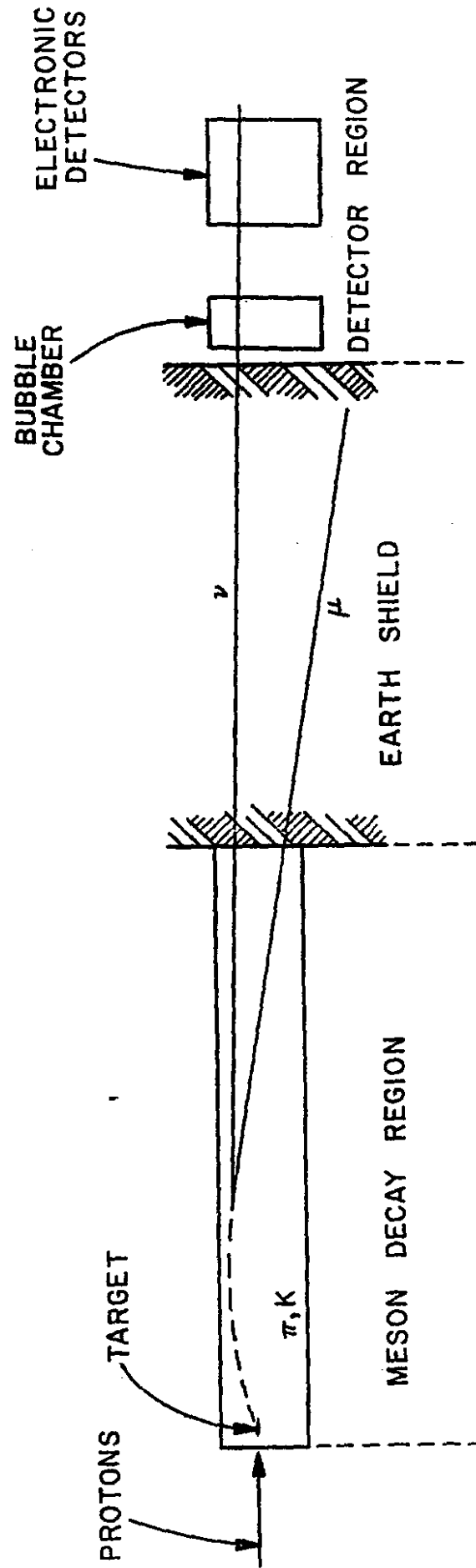
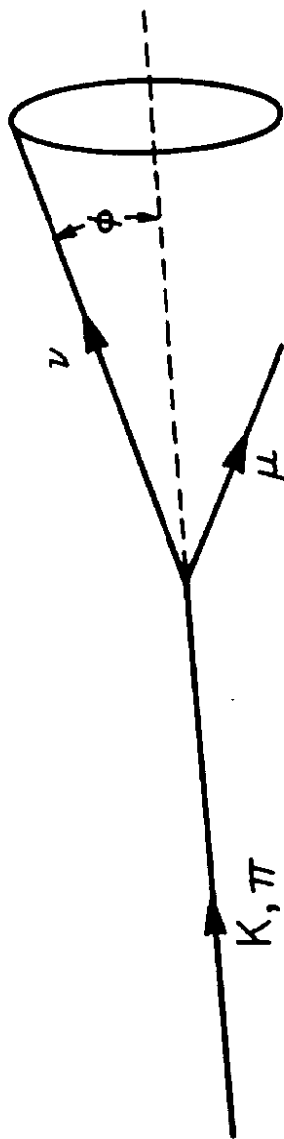
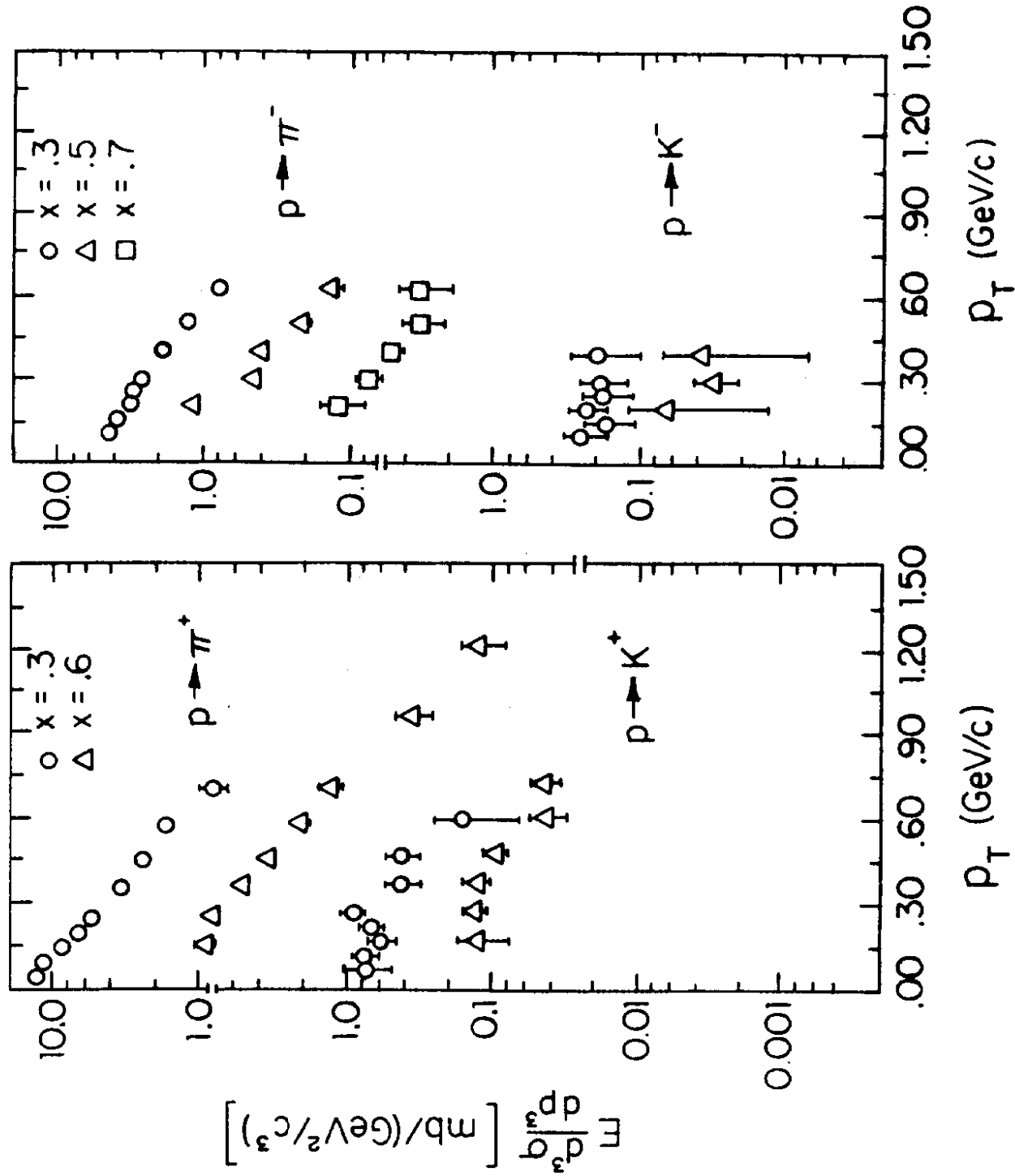


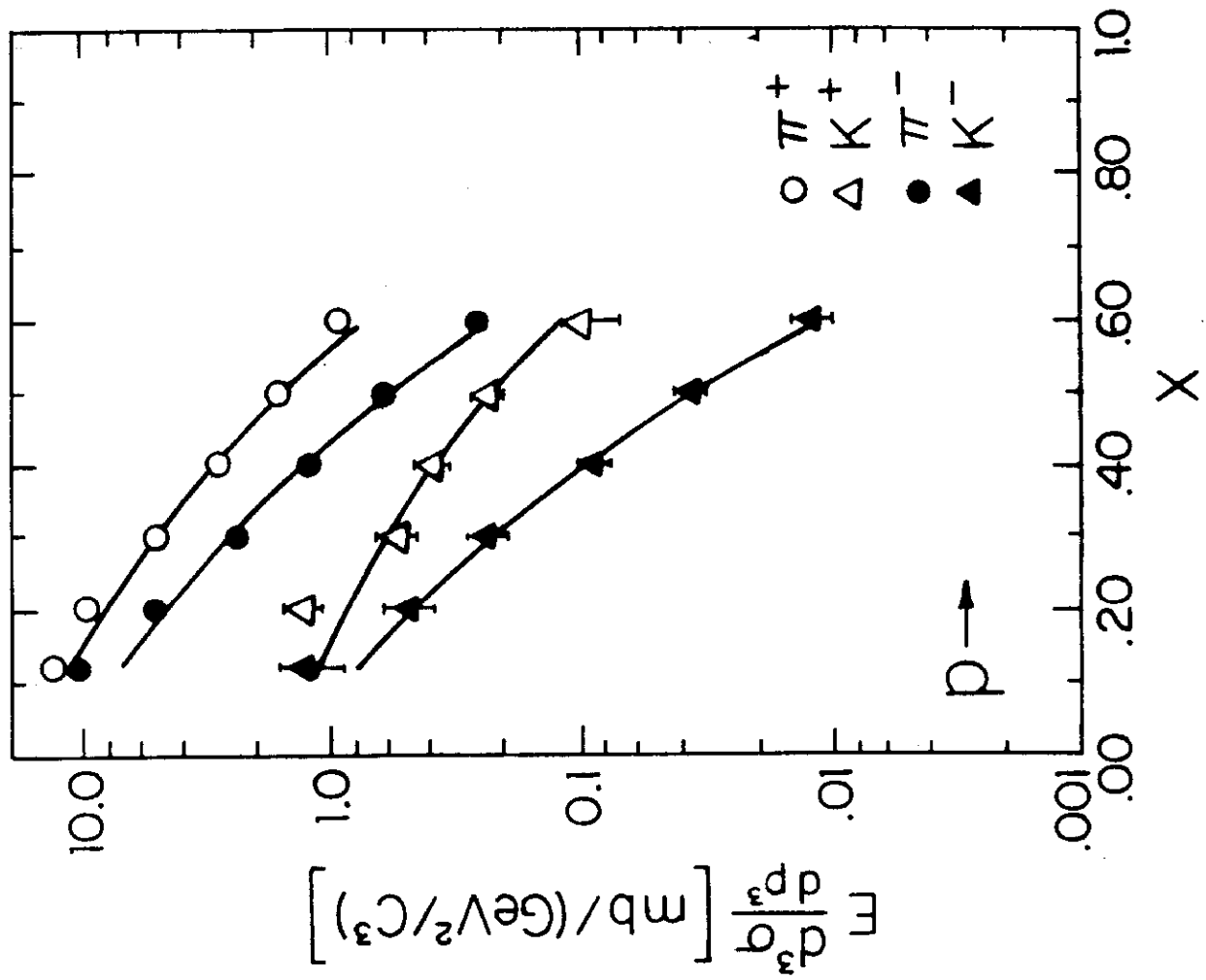
Figure 1. The Fermilab Neutrino Area



2. A meson decays into a muon and an antineutrino. The angle the neutrino trajectory makes with the original meson trajectory is labelled ϕ and is determined uniquely by the neutrino energy and the meson momentum. The decay neutrinos of a given energy form a cone about the extension of the meson trajectory.

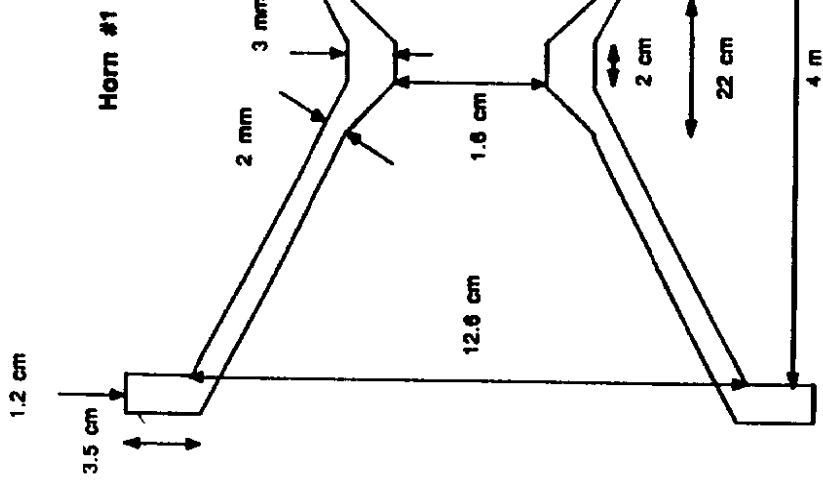
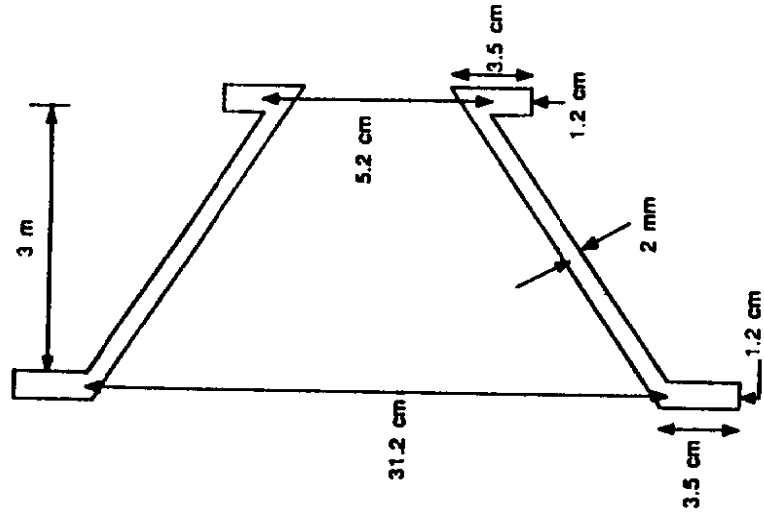


3. The transverse momentum distribution of pions and kaons produced in a hydrogen target by 100 GeV protons.

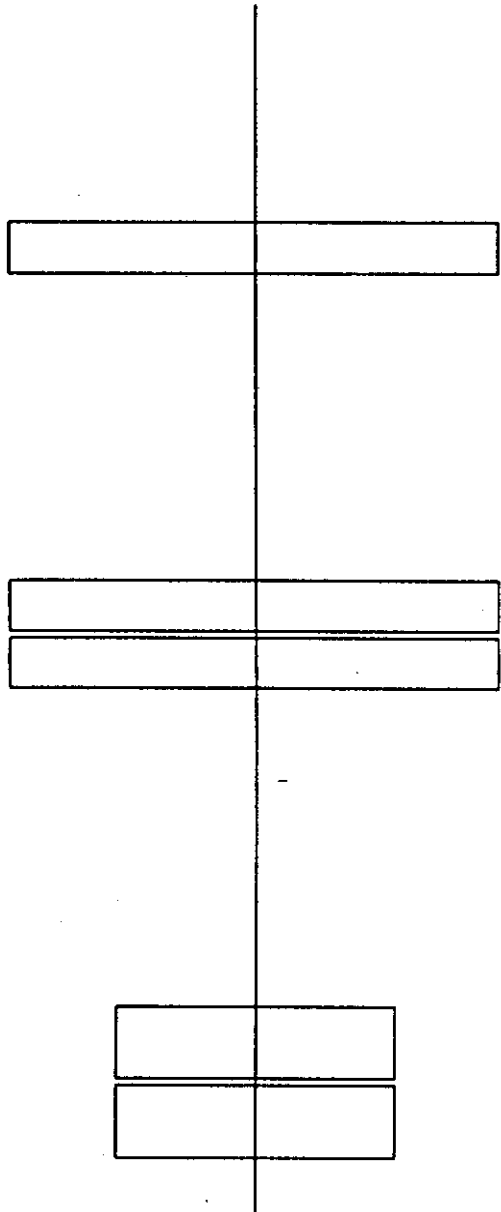


4. The longitudinal momentum distribution of pions and kaons produced in a hydrogen target by 175 GeV protons.

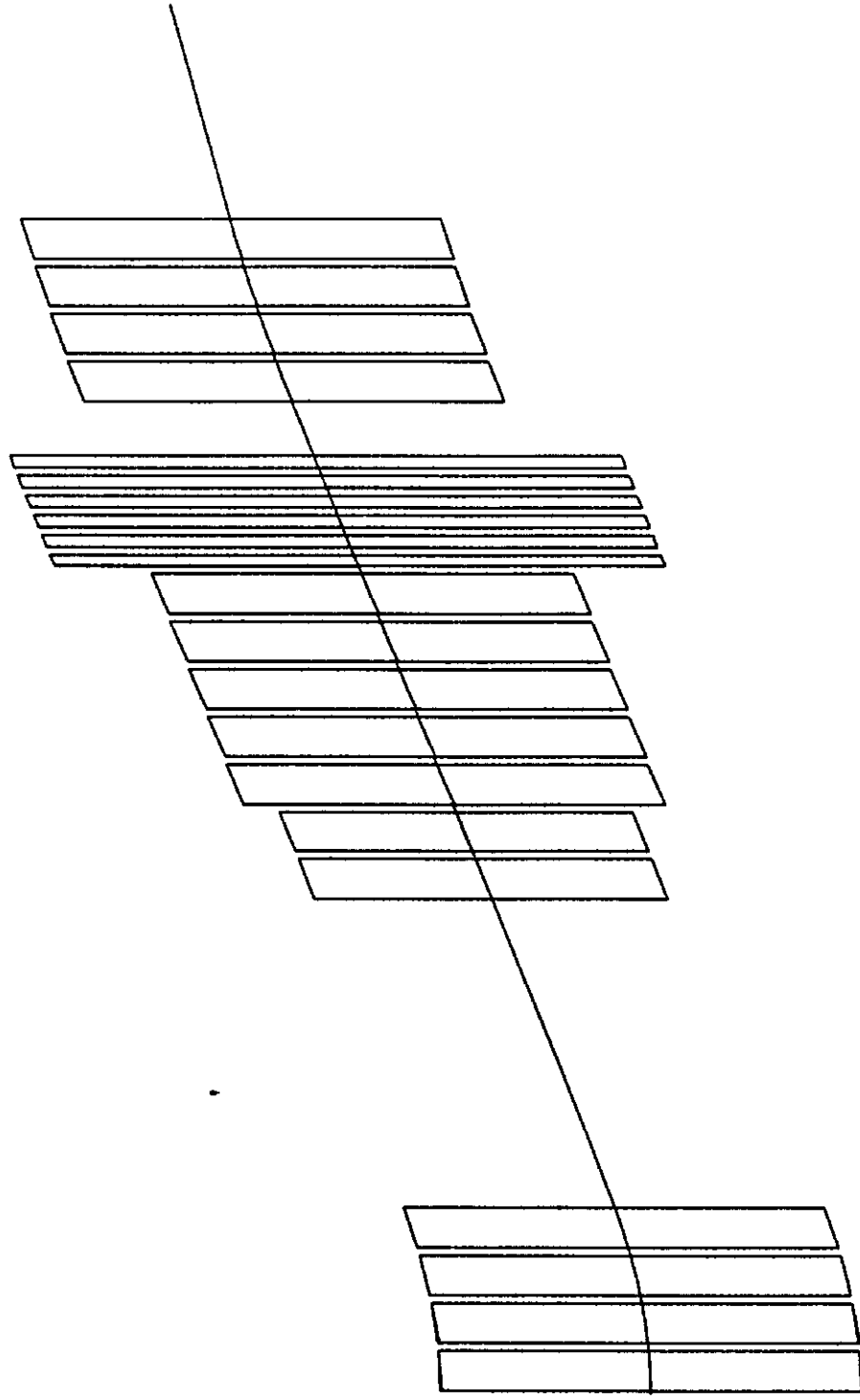
Horn #2



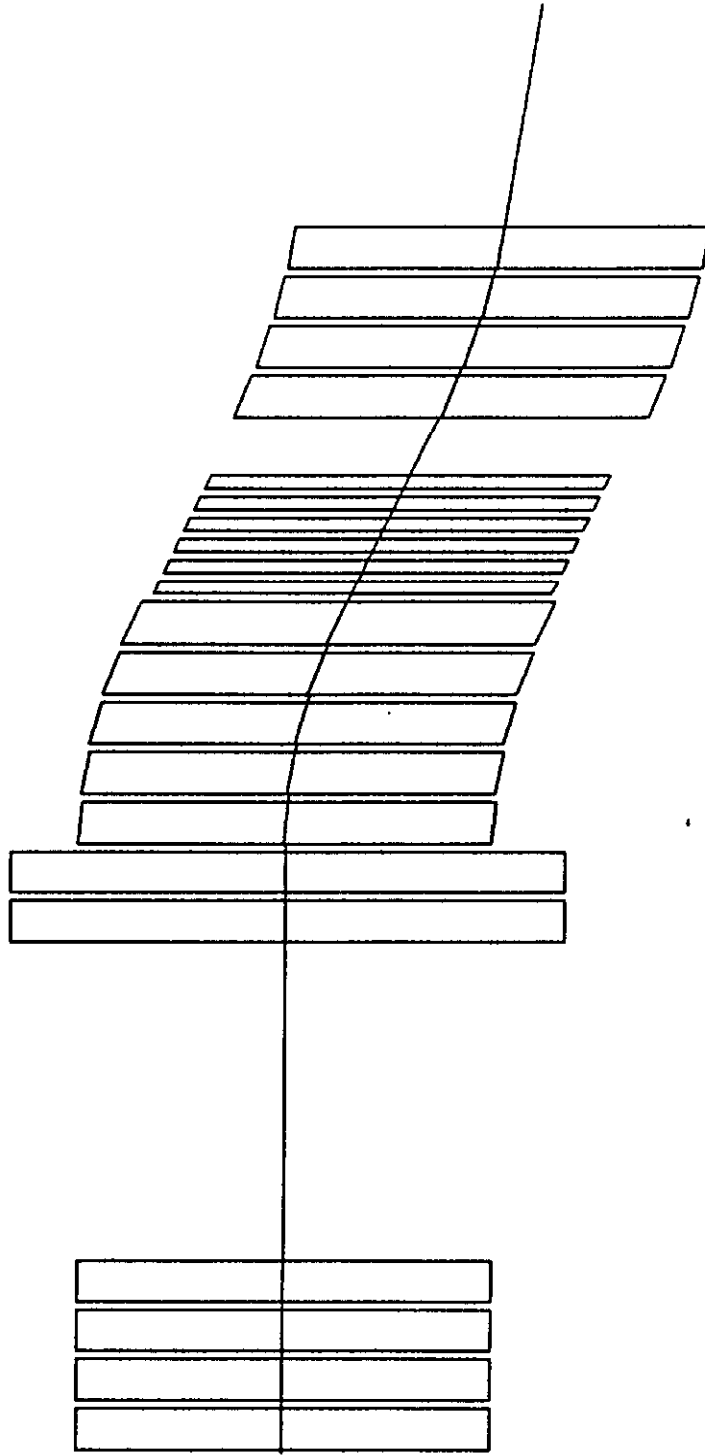
5. A longitudinal cross section of a neutrino horn. Current is passed through the horn from left to right, resulting in a magnetic field coming out of the paper above the horn and going into the paper below it.



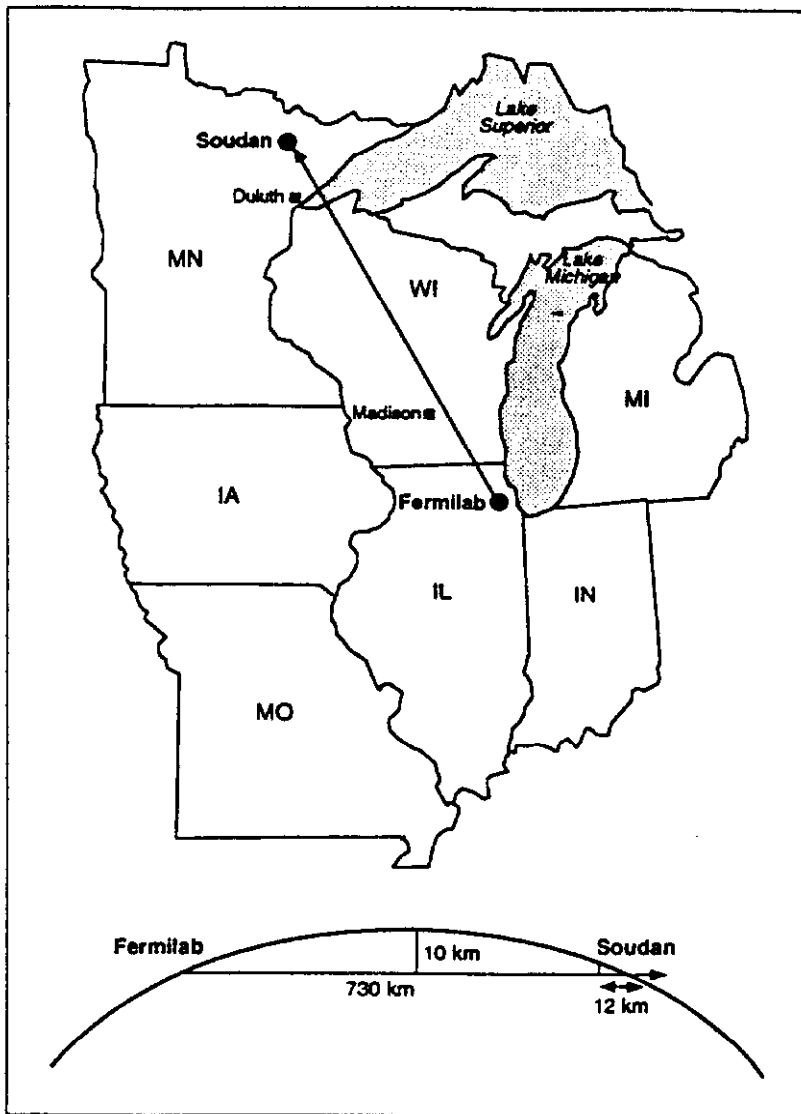
6. The Fermilab neutrino triplet. The focus is point to parallel in both transverse planes.



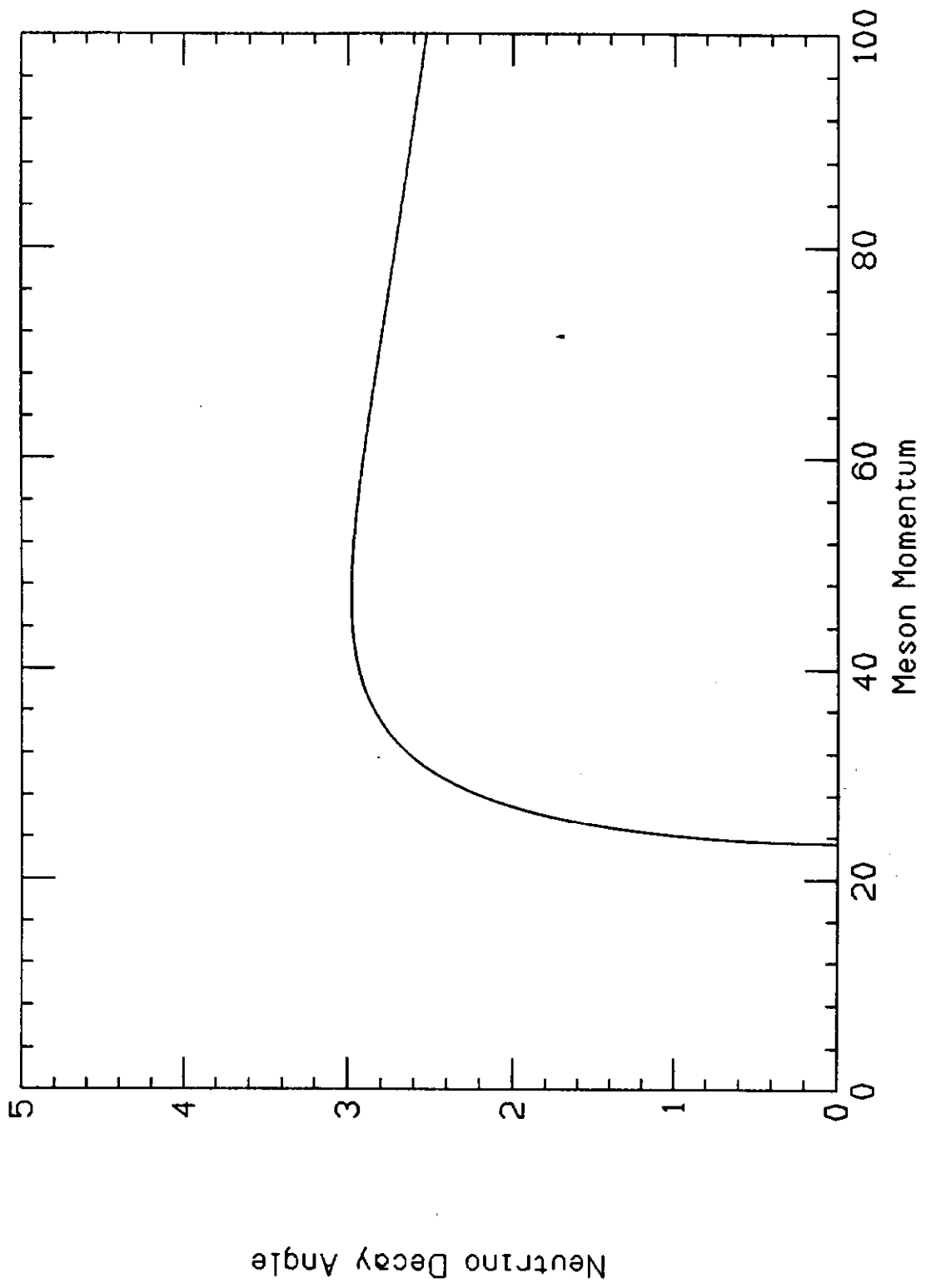
7. The Fermilab dichromatic neutrino beam as seen from above. Only the horizontally bending set of magnets produces a visible deflection in the reference trajectory.



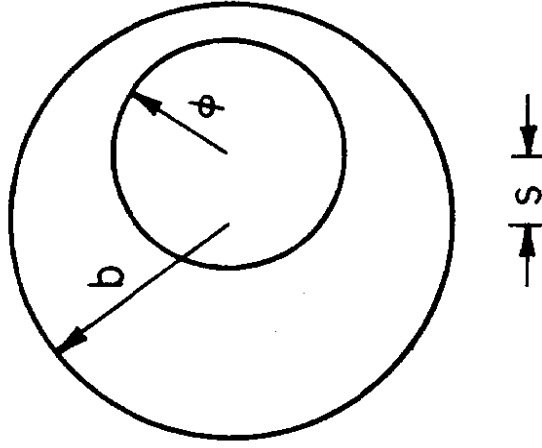
8. The Fermilab dichromatic neutrino beam as seen from the side. Only the vertically bending set of magnets produces a visible deflection in the reference trajectory.



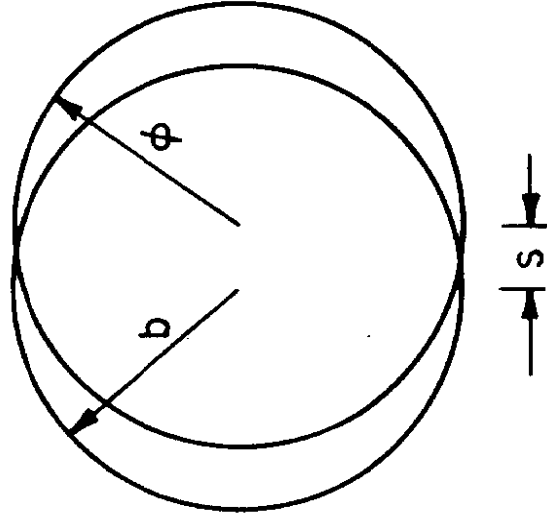
9. The proposed layout of the facility for detecting neutrino oscillations. The detector is quite removed from the source. The curved object at the bottom of the figure represents the surface of the earth.



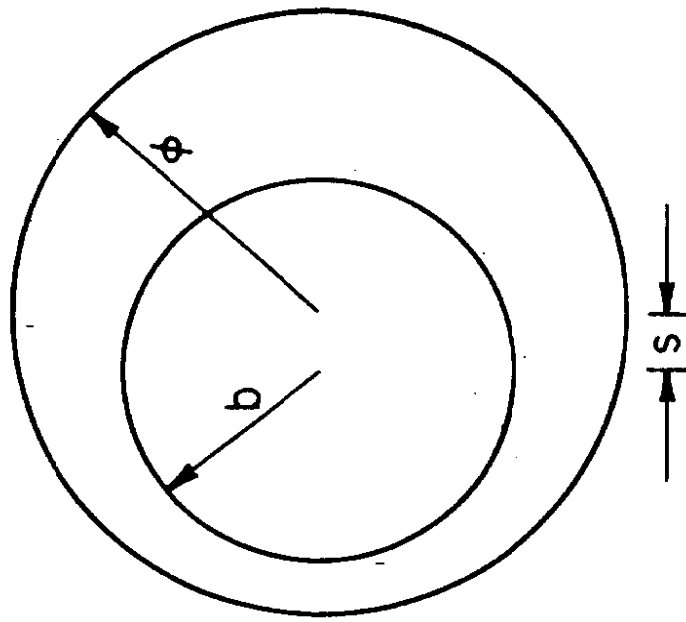
10. The neutrino decay angle ϕ as a function of meson momentum for a given neutrino energy.



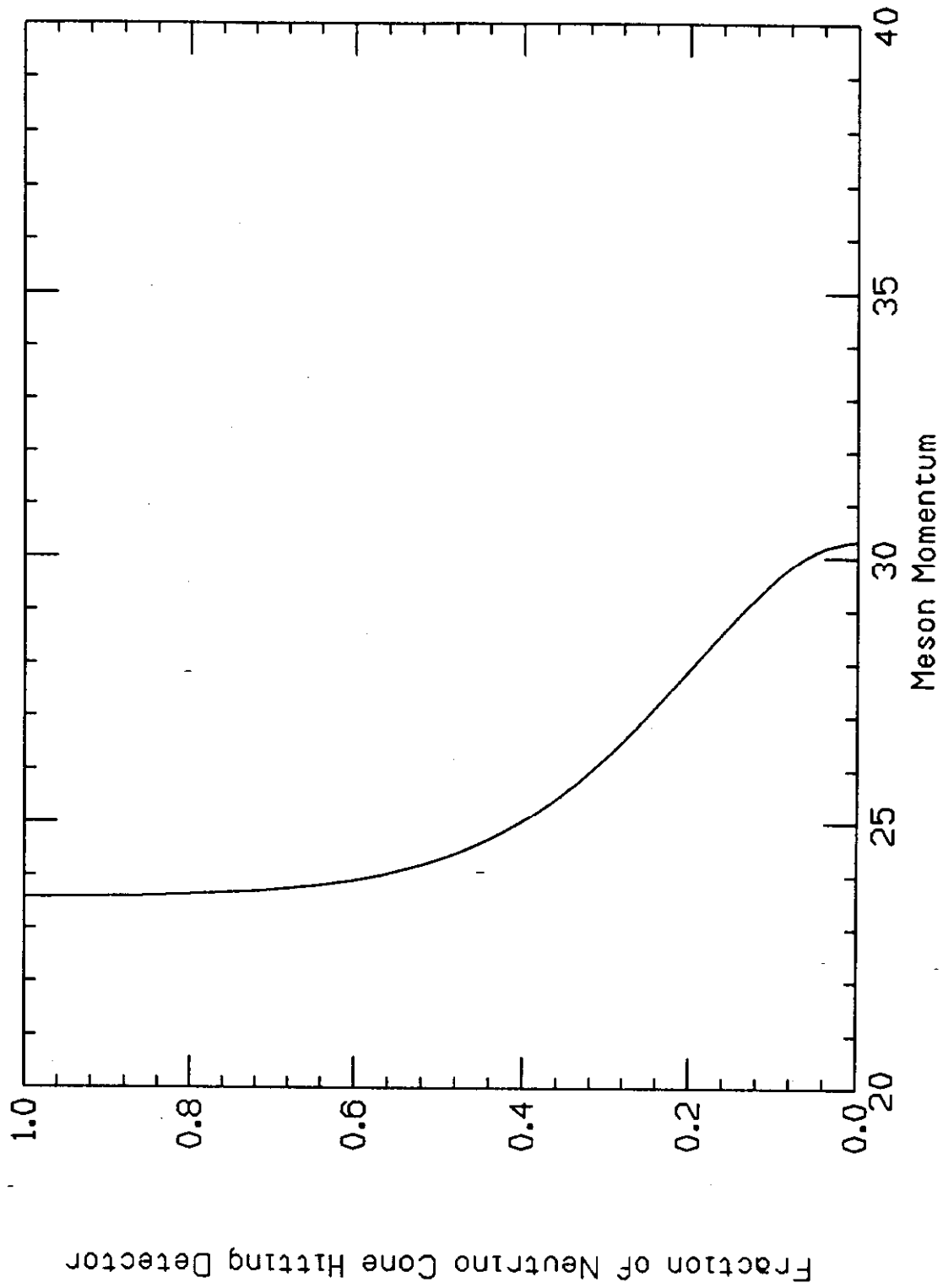
11. The neutrino decay cone at the plane of the detector. The projected meson direction lies inside the detector. The angle ϕ is sufficiently small that the neutrino decay cone also lies entirely inside the detector.



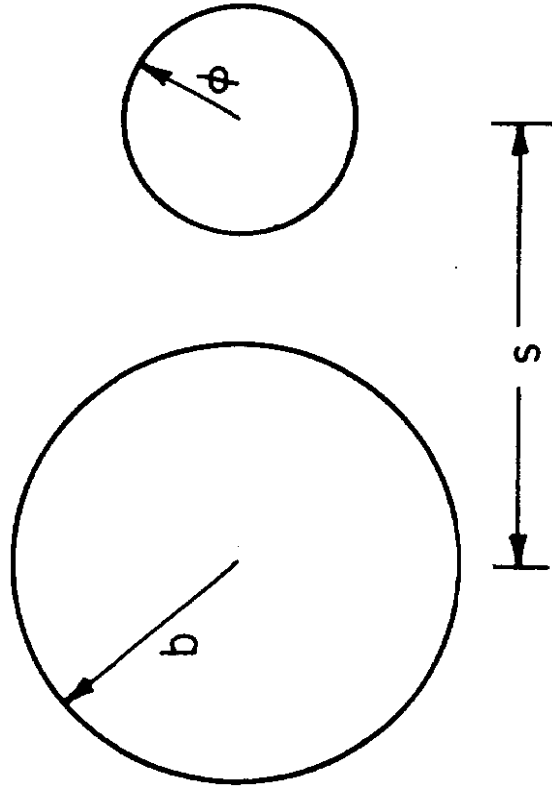
12. The neutrino decay cone at the plane of the detector. The projected meson direction lies inside the detector. The angle ϕ is of such a size that the neutrino decay cone partially intersects the detector.



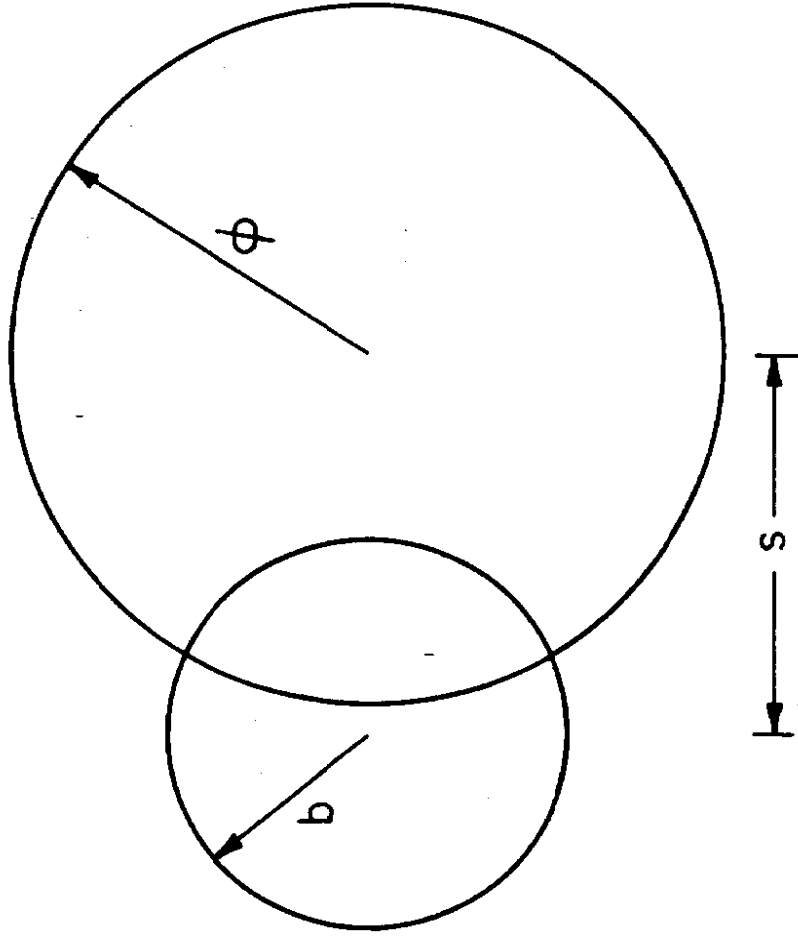
13. The neutrino decay cone at the plane of the detector. The projected meson direction lies inside the detector. The angle ϕ is sufficiently large that the neutrino decay cone encloses, but lies entirely outside of the detector.



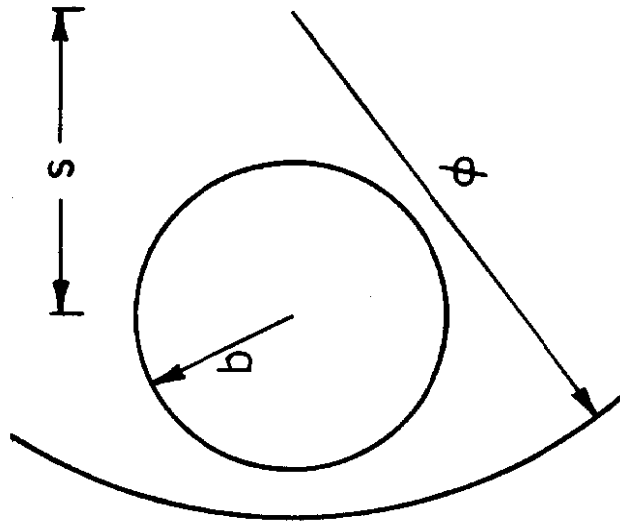
14. The fraction of the cone intersecting the detector as a function of meson momentum. The cone center is inside the detector.



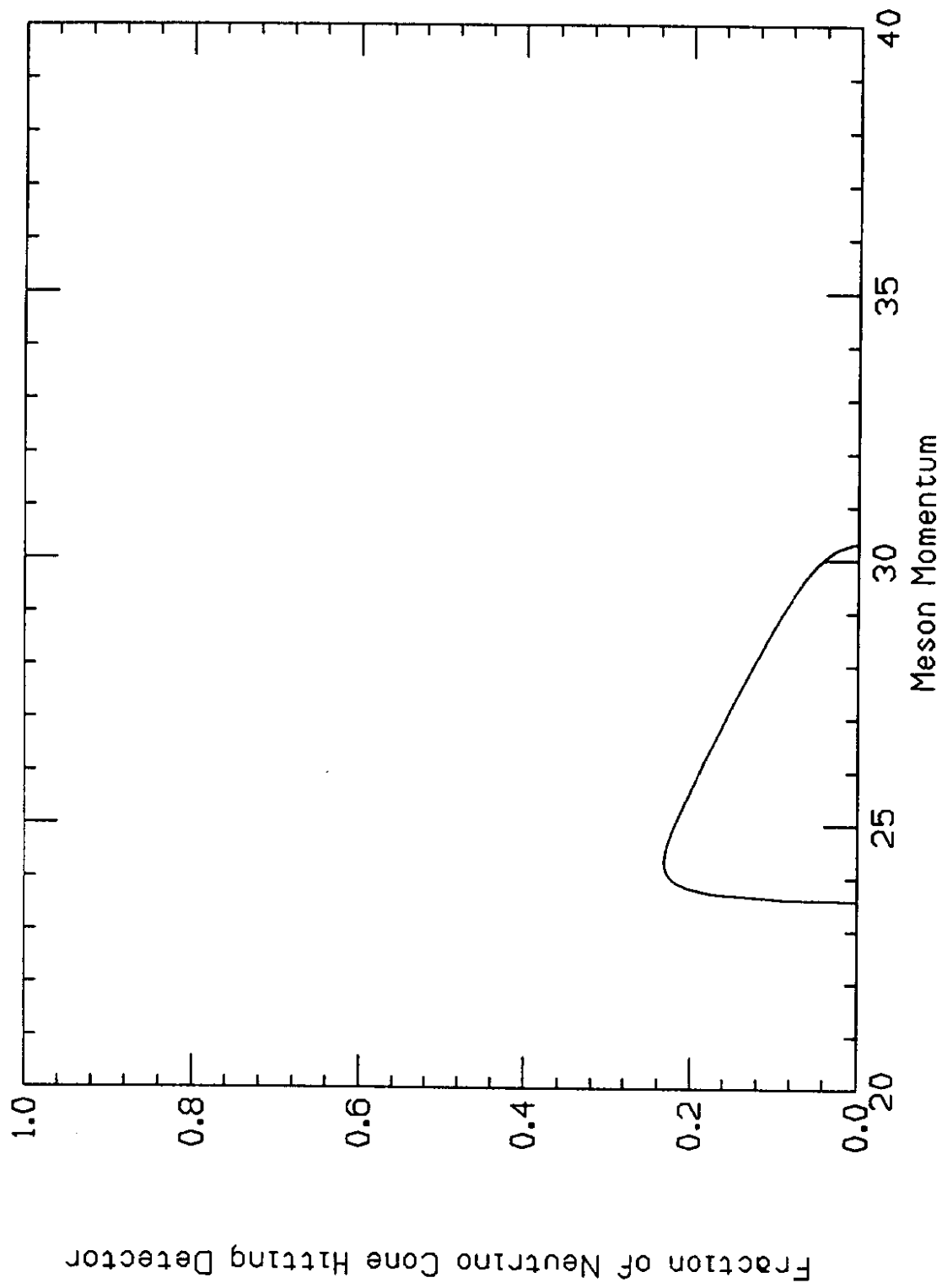
15. The neutrino decay cone at the plane of the detector. The projected meson direction is outside the detector. The angle ϕ is sufficiently small that the neutrino decay cone lies entirely outside the detector.



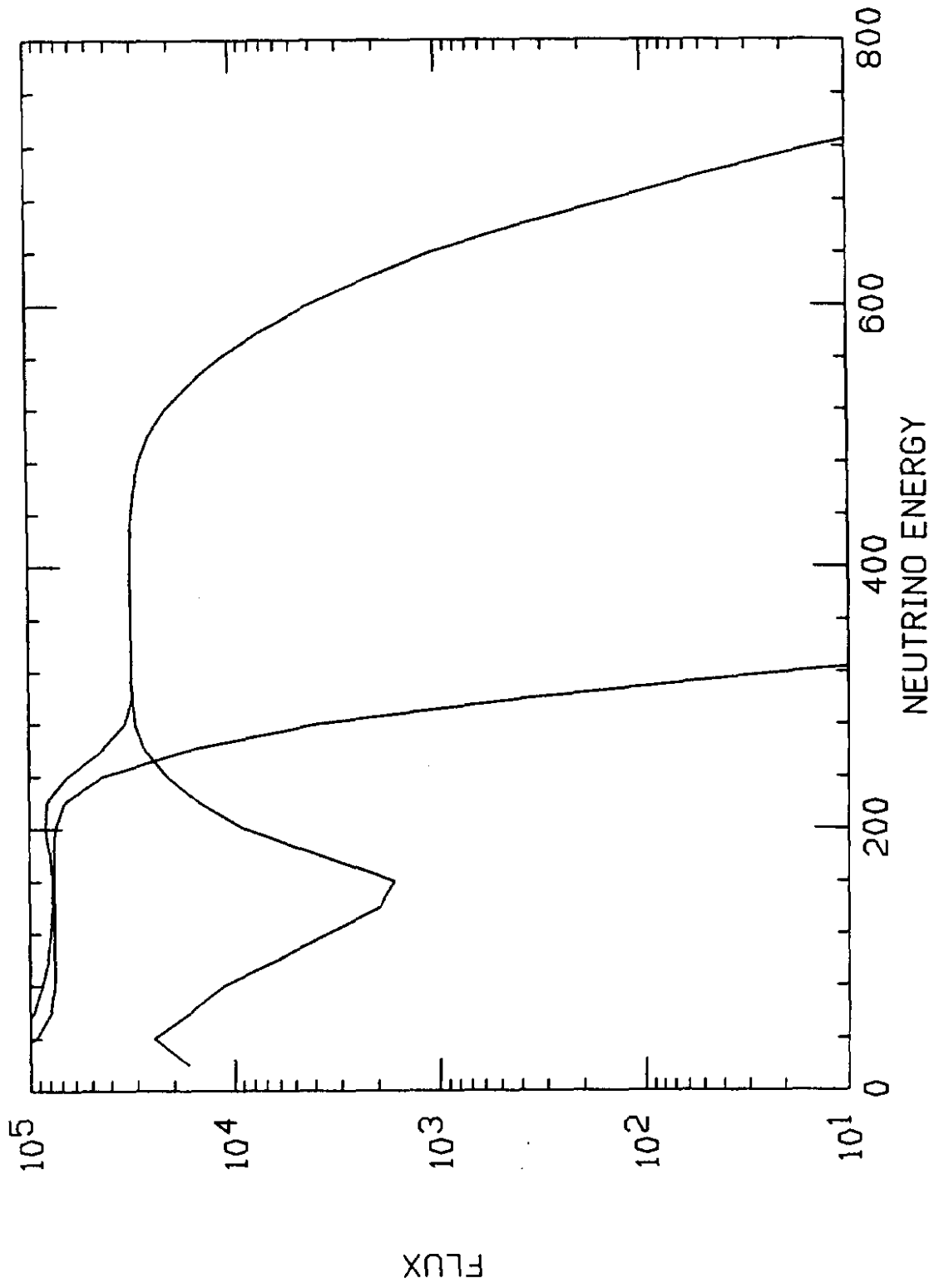
16. The neutrino decay cone at the plane of the detector. The projected meson direction is outside the detector. The angle ϕ is of such a size that the neutrino decay cone intersects the detector.



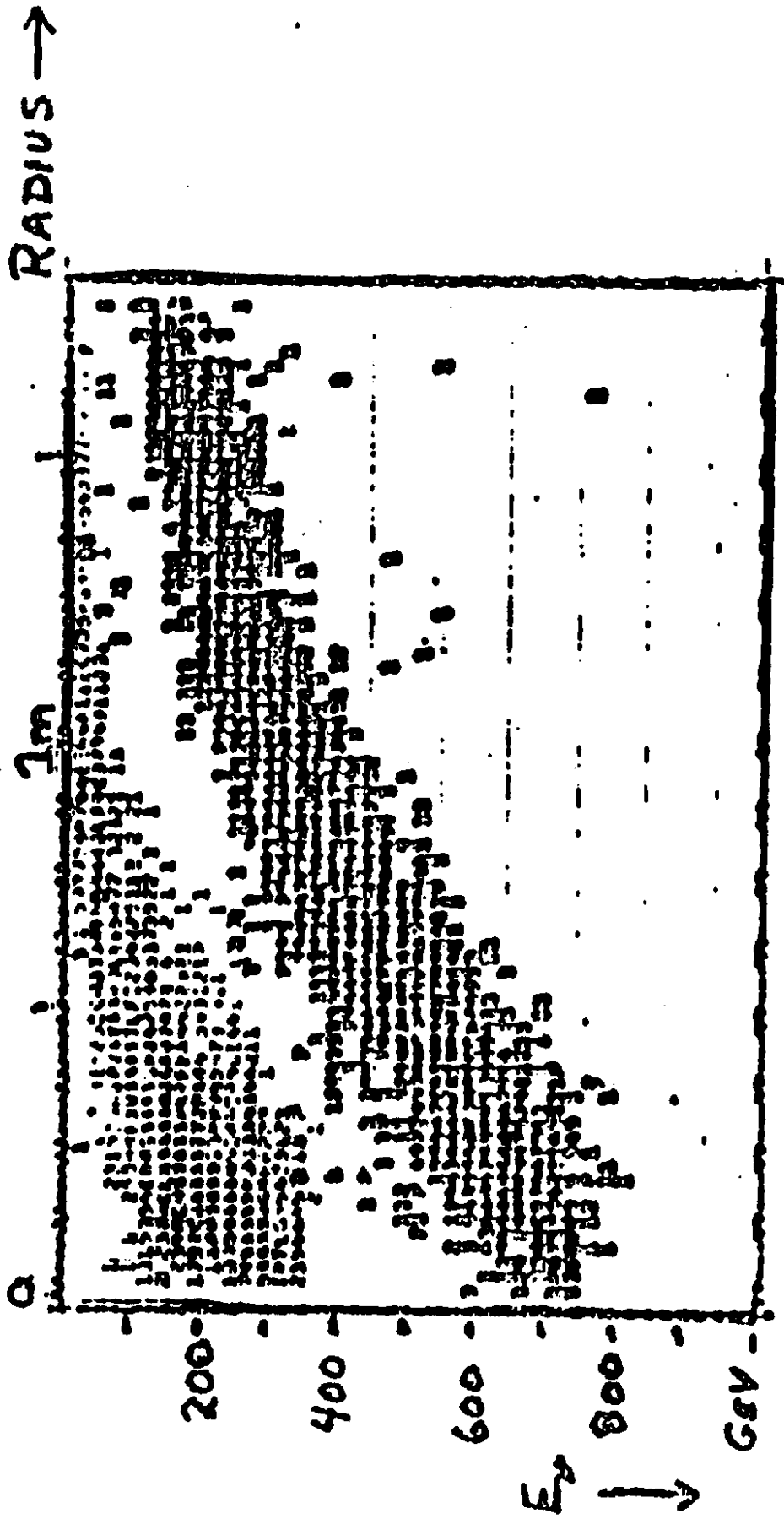
17. The neutrino decay cone at the plane of the detector. The projected meson direction is outside the detector. The angle ϕ is sufficiently large that it encloses, but lies entirely outside the detector.



18. The fraction of the cone intersecting the detector as a function of meson momentum.
The cone center is outside the detector.



19. A graph of neutrino flux vs neutrino energy. Curves are shown for the pion contribution alone, the kaon contribution alone, and for the sum. For reasons explained in the text, the curve from pion production occurs at lower energy than that from kaon production.



20. A plot of neutrino energy vs radial position in the detector. Neutrinos produced from pions and neutrinos produced from kaons fall in different bands. The neutrinos from kaon decay have the higher energy for a given detector radius.